10^{th} International Conference on Fracture Mechanics of Concrete and Concrete Structures
FraMCoS-X
G. Pijaudier-Cabot, P. Grassl and C. La Borderie (Eds)

https://doi.org/10.21012/FC10.233164

NUMERICAL SIMULATION OF HS-SHCC UNDER QUASI-STATIC TENSILE LOADING

Alaleh Shehni[*†], Ulrich Häussler-Combe[*‡], Iurie Curosu[§ϒ], Ting Gong[§□]and Viktor Mechtcherine[§◊]

[*]Technische Universität Dresden
Institute of concrete structures, D-01062 Dresden, Germany
[†]e-mail: alaleh.shehni@tu-dresden.de

[‡]e-mail: ulrich.haeussler-combe@tu-dresden.de

[§]Technische Universität Dresden
Institute of Construction Materials, D-01062 Dresden, Germany
[ϒ]e-mail: iurie.curosu@tu-dresden.de

[□]e-mail: ting.gong@tu-dresden.de

[◊]e-mail: viktor.mechtcherine@tu-dresden.de

Key words: Fiber Reinforced Concrete, Strain-hardening, SHCC, Discrete fiber modeling, FEM

Abstract. This paper presents a study for modelling the behaviour of high strength SHCCs (strain-hardening cement-based composites) made with high performance polymer fibers under quasi-static tensile loading. High density polyethylene fibers are modelled explicitly and distributed randomly in a two-dimensional model. Single fiber pull-out test result is used for micromechanical characterization of bond strength. Load test simulations are conducted with in-house program CaeFem and comparisons are made with experimental results. Several sensitivity analyses performed based on different fiber contents and notches located in the mid-height of a dumbbell specimen.

1 INTRODUCTION

Nowadays, addition of a small volume of short fibers is a well known strategy to increase the ductility and toughness of cementitious matrices besides optimization of crack opening while the pure cementitious composites have shown quasi-brittle behavior with undesirable typical large cracks under tensile loading condition [1–4]. Strain-hardening cement-based composites (SHCC), which are a special class of fiber reinforced concretes, are able to develop controlled multiple cracks while subjected to incremental tensile loading condition [5]. In previous studies, the contribution of short fibers in overall behavior and specifically in post-cracking phase is considered with smeared crack formulation or crack bands within finite element method [6–8].

2 2D EXPERIMENTAL PROGRAM

2.1 Materials

The modelled composite is a high-strength SHCC made with ultra-high molecular weight polyethylene (UHMWPE; or shortly PE) Dyneema SK62 fibers, produced by DSM, the Netherlands [9]. This material was investigated in detail in previous works by the authors [10]. The used Dyneema fibers have an average di-

ameter of 20 μm and their cut-length is 6 mm. Composites with a volume ratio of short fibers of 1% and 2% were analyzed.
The high-strength matrix was specifically developed for an adequate interaction with the hydrophobic PE fibers [11, 12]. For that, the matrix had to exhibit a high packing density and strength. Furthermore, to ensure a steady-state cracking in the strain-hardening phase, the matrix should yield a very low fracture toughness [13]. For fulfilling the above enumerated micromechanical conditions, the matrix has a high cement content, low water-to-binder ratio, small amount of fine sand and no coarse sand or aggregates. Despite its high compressive strength and density, the cementitious matrix has a rather low tensile strength and a pronounced brittleness [11], which is advantageous with respect to a pronounced strain-hardening and multiple cracking in the resulting SHCC.
The bond properties of the PE fibers in the high-strength cementitious matrix are given in [10,12] and is characterized by slip-softening and complete pullout of the fibers with embedment lengths of up to 3 mm. The bond properties were adjusted with respect to a maximum possible exploitation of fiber's tensile strength at the same time avoiding excessive fiber rupture during crack opening, which would lead to a brittle fracture.

2.2 Specimen production and testing

For the purpose of 2D FEM simulations of SHCC with a discrete fiber representation, special dumbbell-shaped specimens with a very thin cross-section in the gauge portion were designed and produced, see Figure 1a. The molds consist of plastic elements assembled together through bolted connections. The small thickness was achieved by pressing profiled elements into the molds filled with fresh SHCC until the purposefully dimensioned spacers impeded any further displacement. The pressed material was squeezed towards the open ends of the molds, in this was aligning the fibers longitudinally. The predominantly longitudinal orientation of the fibers was also a desired aspect with regard to the performed numerical simulations.
The specimens were cured for 27 days in the molds. The curing was done in sealed plastic bags in a climatic chamber with constant temperature (20°C) and humidity (65°C) conditions. This curing procedure allowed minimizing the development of shrinkage cracks, which could be promoted by the high cement content in the investigated SHCC as well as large surface area and small cross-section of the samples.
Prior to testing, the specimens were extracted from the mold assembly together with the profiled mold elements. The latter were connected to each other by long threaded rods at the specimen ends, as shown in Figure 1b. The extraction was done for applying the speckle pattern necessary for the optical monitoring of the deformations during the test as well as for cutting the notches. Prior to testing, these elements were bolted back to the specimens and confined the samples during the gluing process.

Figure 1: a) Naked unnotched SHCC specimen, b) specimen fixed in the testing machine. The lateral confining elements were removed shortly before load initiation.

The specimens had a cross-section of 3.5 mm x 40 mm in the gauge portion and 40 mm x 40 mm at their ends. The total specimen length was 250 mm with a gauge length of 100 mm. The transition zones between the large cross-sections at samples' ends and the thin gauge portions were 35 mm long. These geometrical proportions ensured a proper fixation of the samples in the testing machine on one hand, and failure localization in the gauge portion, on the other.
Figure 1b shows a specimen fixed in the testing machine together with the confining mold elements. Non-rotatable boundaries were ensured by gluing the specimens in thick steel rings, which were bolted to the machine cross-members. The same testing conditions were used by the authors in the previous works on common specimen geometries [10, 12]. The tests were performed in a hydraulic testing machine Zwick 1200 in a displacement controlled mode with a displacement rate of 0.05 mm/s. Notched and un-notched specimens were tested. The notches were cut in the middle on both sides of the samples. The results on notched specimens with a fiber content of 2% are shown in Figure2.

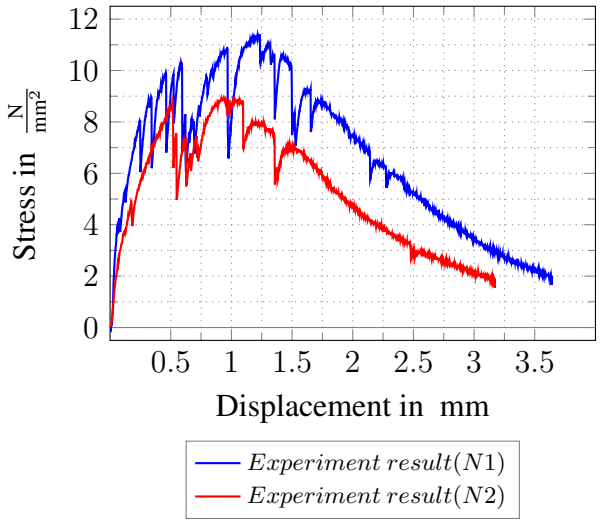

Figure 2: Experimental results on notched specimens with a fiber content of 2%

3 NUMERICAL SIMULATION

3.1 2D random mesoscopic model

The 2D SHCC tensile models were analyzed with in-house program CaeFem which is based on finite element simulation. The distribution of discrete fibers are randomly considered in the model. Since localization and development of cracks will be occurred in the notched area, for numerical simulation, special attention will be given to the middle of the dumbbell specimen. This way the modeling effort will be efficient and the required computational time will be optimized. Each components of cement-based composites should be modeled separately in mesoscopic scale. The model is in the context of plane-stress and 2D truss element represents embedded fibers [14]. Truss nodes and neighboring continuum nodes are coupled by special bond elements, which are stiff in normal direction to avoid overlapping and flexible in longitudinal direction according to the governing bond-slip law. Linear elastic material models, with corresponding mechanical properties shown in Table1, are used for truss elements and bond elements.
In Figure4, Geometry of dumbbell specimen, random distribution of longitudinally aligned fibers and FEM mesh are shown. For geometry, boundary condition and acting load on notched model see Figure3. Material properties used for simulation are shown in Table1.
It is noteworthy to mention that the experimental specimens are slender and several micro-cracks have been observed before performing the test. In order to consider the effect of these initial cracks in the numerical simulation, based on the experimental results shown in Figure2, the Young's modulus of cementitious material is decreased by the factor of 3 in the numerical analyzes.

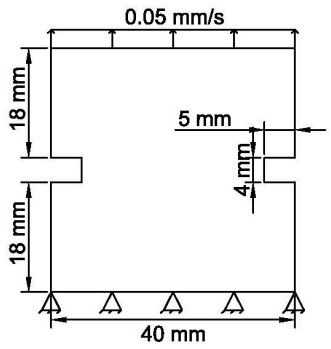

Figure 3: Geometry, boundary condition and acting load

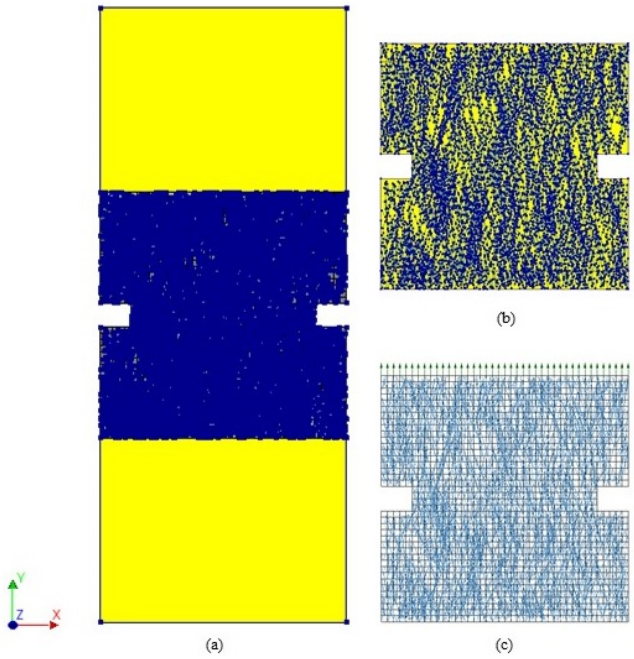

Figure 4: a) Geometry of dumbbell specimen, b) random distribution of longitudinally aligned fibers in notched model, c) FEM mesh

Table 1: Material properties used for simulation

Concrete	Young's modulus	[N/mm^2]	29000
	Poisson's ratio		0.2
	Tensile strength	[N/mm^2]	3.8
	Crack energy	[N/mm]	0.1
	Critical crack width	[mm]	0.1
Fiber	Fiber Young's modulus	[N/mm^2]	80000
	Fiber diameter	[mm]	0.02
	Fiber length	[mm]	6
Bond	Bond strength	[N/mm^2]	3.0
	Slip with bond strength	[mm]	0.1

3.2 Continuum material model

A particular type of damaged material model is used for representing the response of the continuum medium. This particular damaged model consist of elastic zone up to Rankine criteria which the largest principle strain of a continuum element exceed the threshold value corresponding the uniaxial tensile strength, the respective element will be extended with strong discontinuity approach (SDA). The relation between crack normal traction and crack width is described by a quadratic function, see Figure5. The starting point in the loading phase is defined by the limited uniaxial tensile strength and the end point depends on the prescribed crack energy which is equal to area of the graph in the loading condition. A fixed crack approach is assumed as first approach while the crack direction is assumed as normal to direction of the largest principle strain and the crack anchor point is placed the element's center (See Figure 6). The crack formation is dependent on the loading history. Since the SDA-approach with a crack-traction law is able to recover the energy in un/re-loading phases, there would be no need for any special regularization to capture the tensile softening behavior of concrete in FEM displacement field.

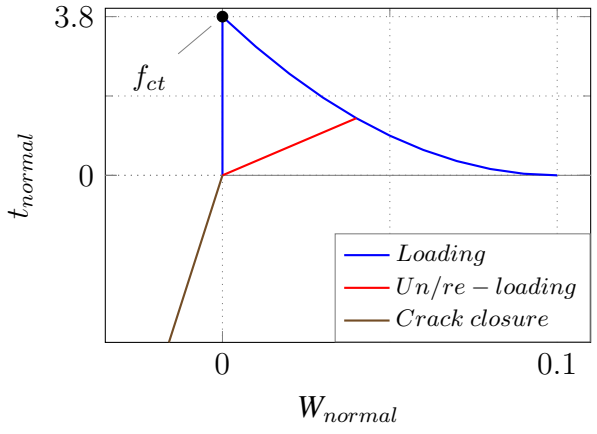

Figure 5: Constitutive model for softening in matrix, [*Crack normal traction* vs *Crack width*]

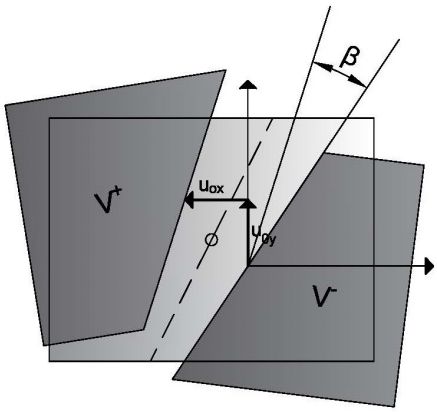

Figure 6: Extended continuum element with SDA

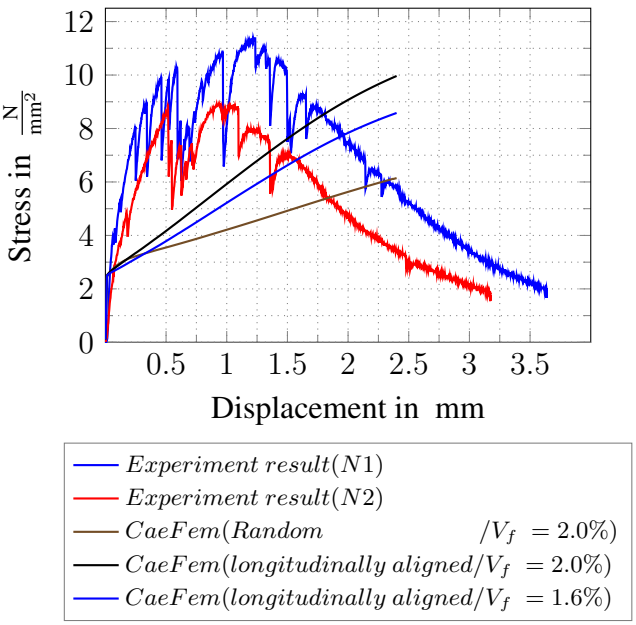

Figure 7: Results comparison, [*longitudinally aligned fiber orientation* vs *Random fiber orientation* and *Volume fraction 2.0%* vs 1.6%]

4 ANALYSIS RESULTS AND PARAMETERIC STUDY

Our interest at this stage of the simulation is to capture the overall response of the specimen. The observed saw edges from the experimental results, which are due to initiation and propagation of the damage in the model and redistribution of energy in the specimen, will not be investigated(See Figure7).
This localized behavior could vary due to random distribution of fibers, the cementitious quality and set-up of the equipment.
Several sensitivity analysis have been performed and results are compared to corresponding experimental results for notched specimens with a fiber content of 2%.

4.1 The effect of random distribution field and volume fraction

In Figure7 the effect of fiber orientation and volume fraction of fiber in model are investigated, it is observed that longitudinally aligned orientation of fiber and higher volume ratio increase the ductility and tensile strength of the overall response of the specimen.

Since the production techniques and the thickness of the specimens (≈3.5 mm) led to an almost uniaxial fiber orientation, model with longitudinally aligned fibers and a fiber content of 2% is used for the next sensitivity analyses.

4.2 The effect of ultimate bond - slip stress

It should be noted that result, shown in Figure7, present a constant increase because no failure in bond material model, fiber material model and no complete pull-out for truss element is considered. Additional nonlinearity is introduced to the existing bonding material behaviour in order to address ultimate bond-slip stress(see Figure8).
The results of new material model for bond elements are shown in Figure9. It is observed that decreasing the ultimate bond-slip stress will shorten the hardening phase and decrease the ductility in the overall response of the specimen.

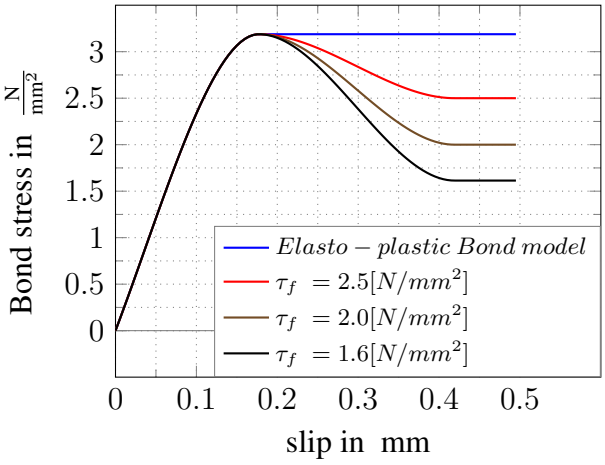

Figure 8: Constitutive model for bond, [τ_f is *Ultimate bond-slip stress*]

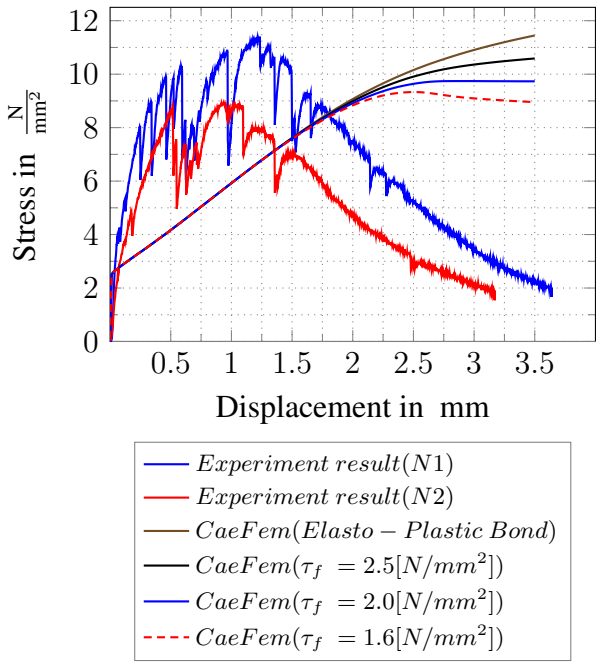

Figure 9: Results comparison, [With different Ultimate bond-slip stress]

4.3 The effect of fracture energy

The area under loading part shown in Figure5 represents the fracture energy of continuum element. A sudden drop is observed in start point of hardening phase when the fracture energy parameter is decreased by a factor of 0.2 and 0.1. It shows that a big number of concrete elements have been failed at the same time due to the low fracture energy, and the model will be stabilized later on by redistribution of stresses into the overall elements.

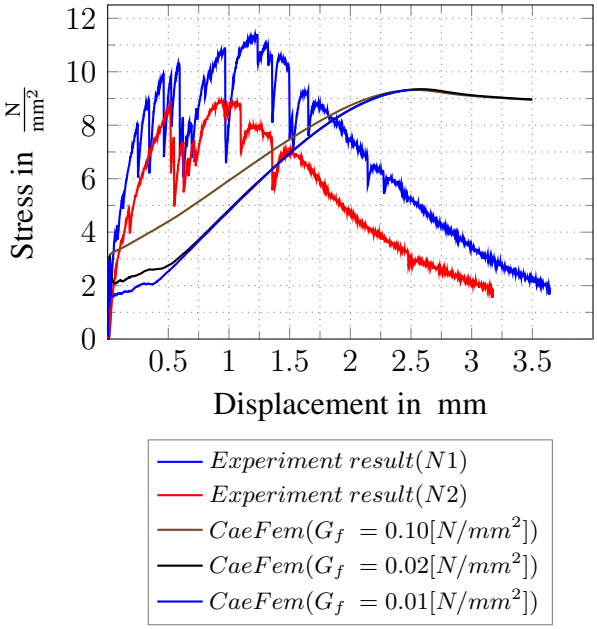

Figure 10: Results comparison, [G_f is *Matrix Fracture energy*]

4.4 The effect of ultimate fiber strength

For modeling the rupture of fibers in the simulation, a multi-linear elastic material model has been assigned to truss elements as preliminary approach. Based on this material model, when the stress in truss elements reaches the ultimate tensile strength, the modulus of elasticity of corresponding fiber will be decreased by a factor of 0.01. From result shown in Figure11, it is observed that by decreasing the ultimate tensile strength of fiber material, the length of hardening phase in overall behavior is decreasing.

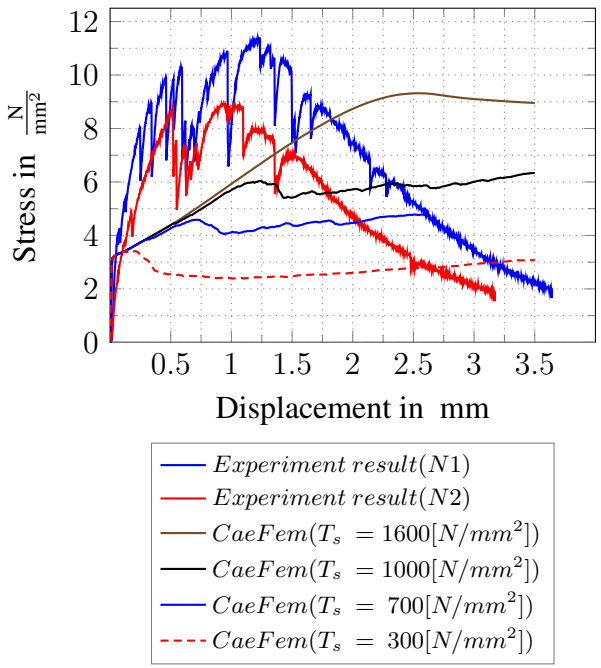

Figure 11: Results comparison, [T_s is *Fiber tensile strength*]

the middle of the sample.

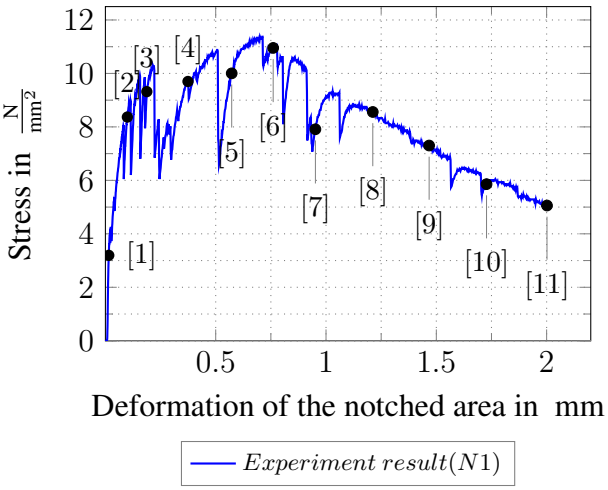

Figure 12: Experimental result- specimen N1, [*Deformation of the notched area*]

4.5 Future developments

As it is mentioned before, the middle notched portions of the specimens are analyzed in terms of crack formation and deformation to reduce the computational effort. The presented diagrams in Figures12,14 are thus corresponding to the deformations in these regions. The deformations were evaluated using Digital Image Correlation in which three virtual calipers were places longitudinally on specimens edges and in the middle. The deformation axes in the following diagrams show the average of the elongation of these profiles.

In Figures13,15, each DIC images presents specific step of crack development in notched area during the experiment and the numbers under the pictures are corresponding to number of points highlighted in Figures12,14 respectively.

Note that the notches did not impede multiple crack formation, which is typical for SHCC [12]. However, they concentrated the crack formation in the middle of the sample and allowed modeling a smaller region of 40 mm length in

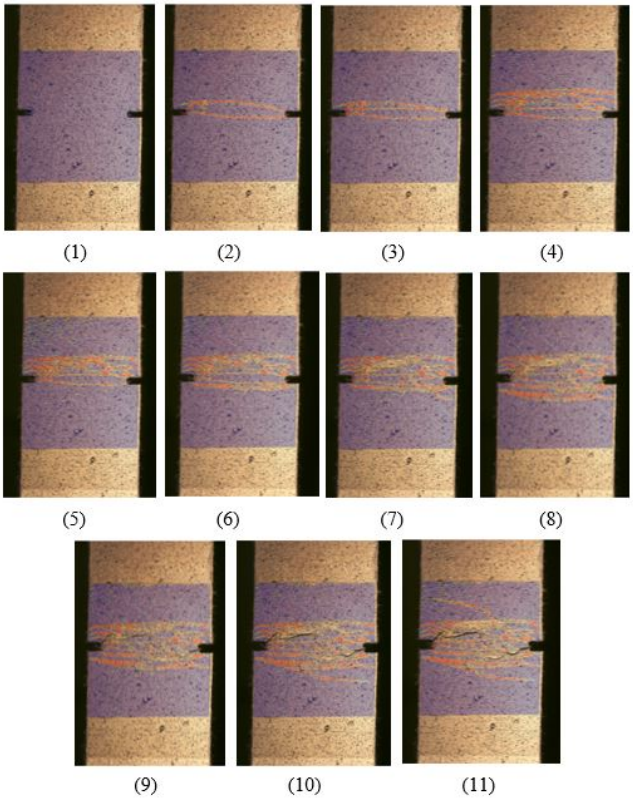

Figure 13: DIC images, crack pattern during tensile test [*Specimen N1*]

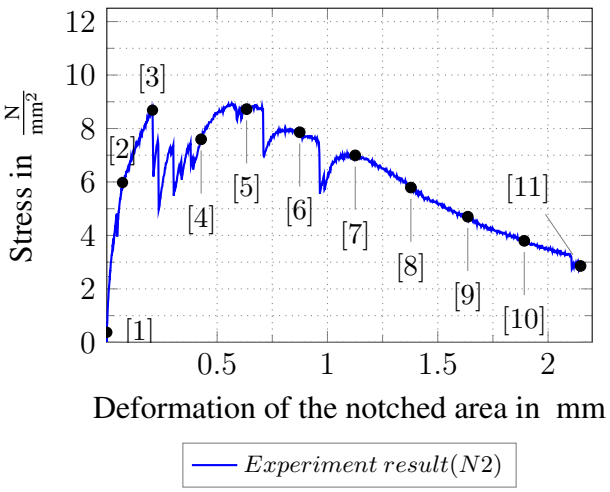

Figure 14: Experimental result- specimen N2, [*Deformation of the notched area*]

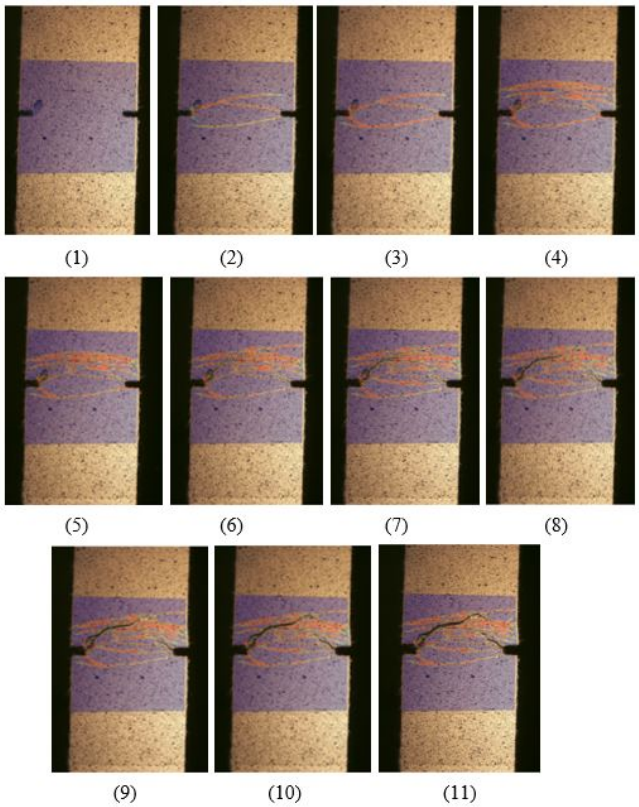

Figure 15: DIC images, crack pattern during tensile test [*Specimen N2*]

Several sensitivity analyses are planned to investigate the effect of continuum mesh sizes and fiber's element length, besides improving the material models to enhance the correlation between experimental and numerical results. The The graphs shown in Figures12,14 will be used as references for validation of further numerical simulations.

5 CONCLUSIONS

This paper represented the modeling strategy for simulation of SHCC specimen made with UHMWPE fibers on a 2D notched specimen. The detailed modeling aspects of matrix, fiber and bonding behaviour are explained. Moreover, several sensitivity analyzes were conducted to highlight the effect of various parameters associated to material properties, volume fraction ratio and orientation of fibers on the overall of response of specimen in the in-house program CaeFem. The progressive failure results from finite element models were compared versus the experimental results.

REFERENCES

[1] Bentur, A. and Mindess, S., 2007. Fiber reinforced cementitious composites. Modern Concrete Technology Series.

[2] Li, V.C., Wang, S. and Wu, C., 2001. Tensile strain-hardening behaviour of polyvinyl alcohol engineered cementitious composite (PVA-ECC), *ACI Materials Journal* **98**:483–492.

[3] Wittman, FH. and van Zijl, G., 2011. *Durability of strain-hardening fiber-reinforced cement-based composite(SHCC)*, Springer, Berlin.

[4] Naaman, AE. and Reinhardt, HW., 1996 *Characterization of high performance fiber reinforced cement composites-HPFRCC*, E FN SPON, London (1-24 pp.).

[5] Li, V.C., 2003. On engineered cementitious composites (ECC): a review of the material and its applications, *Journal of Advanced Concrete Technology* **1**:215–230.

[6] Caner, F.C. Bažant, Z.P. and Wan-Wendner, R., 2013. Microplane model M7f for fiber reinforced concrete, *Engineering Fracture Mechanics* **105**:41–57.

[7] Mihai, I.C. Jefferson, A. and Lyons, P., 2016. A plastic-damage constitutive model for the finite element analysis of fiber reinforced concrete, *Engineering Fracture Mechanics* **159**:35–62.

[8] Bažant, Z.P. and Jirásek, M., 2002. Non local integral formulations of plasticity and damage: A survey on recent results, *Journal of Engineering Mechanics* **128**:1129–1239.

[9] Ultra High Molecular Weight polyethylene Fiber from DSM Dyneema – www.gruschwitz.com

[10] Curosu, I., Liebscher, M., Mechtcherine, V., Bellmann, C., Michel, S. 2017. Tensile behavior of high-strength strain-hardening cement-based composites (HS-SHCC) made with high-performance polyethylene, aramid and PBO fibers, *Cement and Concrete Research* **98**:71–81.

[11] Curosu, I., Mechtcherine, V., Forni, D., Cadoni, E. 2017. Performance of various strain-hardening cement-based composites (SHCC) subject to uniaxial impact tensile loading, *Cement and Concrete Research* **102**: 16–28.

[12] Curosu, I., Mechtcherine, V., Millon, O. 2016. Effect of fiber properties and matrix composition on the tensile behavior of strain-hardening cement-based composites (SHCCs) subject to impact loading, *Cement and Concrete Research* **82**: 23–35.

[13] Li, V.C., Leung, K.Y. 1992. Steady-state and multiple cracking of short random fiber composites. Journal of Engineering Mechanics **118** (11): 2246–2264.

[14] Zienkiewicz, O.C. and Taylor, R.L., 1989. *The finite element method*, Volume 1. London:Mc-Graw Hill.